ACS Observations of a Strongly Lensed Arc in a Field Elliptical

John P. Blakeslee[1], K. C. Zekser[1], N. Benítez[1], M. Franx[2], R. L. White[1,3], H. C. Ford[1], R. J. Bouwens[4], L. Infante[5], N. J. Cross[1], G. Hertling[5], B. P. Holden[4], G. D. Illingworth[4], V. Motta[5], F. Menanteau[1], G. R. Meurer[1], M. Postman[1,3], P. Rosati[6], W. Zheng[1]

ABSTRACT

We report the discovery of a strongly lensed arc system around a field elliptical galaxy in *Hubble Space Telescope* (*HST*) Advanced Camera for Surveys (ACS) images of a parallel field observed during NICMOS observations of the *HST* Ultra-Deep Field. The ACS parallel data comprise deep imaging in the F435W, F606W, F775W, and F850LP bandpasses. The main arc is at a radius of $1\farcs6$ from the galaxy center and subtends about 120°. Spectroscopic follow-up at Magellan Observatory yields a redshift $z = 0.6174$ for the lensing galaxy, and we photometrically estimate $z_{\rm phot} = 2.4 \pm 0.3$ for the arc. We also identify a likely counter-arc at a radius of $0\farcs6$, which shows structure similar to that seen in the main arc. We model this system and find a good fit to an elliptical isothermal potential of velocity dispersion $\sigma \approx 300$ km s^{-1}, the value expected from the fundamental plane, and some external shear. Several other galaxies in the field have colors similar to the lensing galaxy and likely make up a small group.

Subject headings: galaxies: elliptical and lenticular, cD — cosmology: observations — gravitational lensing

1. Introduction

The past decade has witnessed a dramatic growth in both the number of known gravitational lenses, and the astrophysical and cosmological applications for which they have been

[1]Department of Physics & Astronomy, Johns Hopkins University, Baltimore, MD 21218; jpb@pha.jhu.edu

[2]Leiden Observatory, P.O. Box 9513, 2300 Leiden, The Netherlands

[3]Space Telescope Science Institute, 3700 San Martin Drive, Baltimore, MD 21218

[4]Lick Observatory, University of California, Santa Cruz, CA 95064

[5]Departmento de Astronomía y Astrofísica, Pontificia Universidad Catolica de Chile, Santiago 22, Chile

[6]European Southern Observatory, Karl-Schwarzschild-Str. 2, D-85748 Garching, Germany

used. Strong lensing can provide valuable information about the detailed mass structure of intermediate-redshift galaxies (e.g., Rusin, Kochanek, & Keeton 2003). The frequency of lensing, as well as the time delays and image positions as a function of redshift, can be used to constrain the cosmological parameters (e.g., Im et al. 1997, Chae et al. 2002). Of course, lensing also provides the opportunity to study the properties of distant objects with the aid of strong magnification (e.g., Franx et al. 1997).

With its unsurpassed resolution at optical wavelengths, the *Hubble Space Telescope* (HST), has played a central role in the study and exploitation of many lensing systems. The installation of the Advanced Camera for Surveys (ACS) (Ford et al. 2002), with its higher resolution, greater sensitivity, and wider field, has made *HST* a yet more powerful tool for gravitational lensing studies. Here, we present our analysis of a strongly lensed arc serendipitously discovered around a field elliptical using ACS. We adopt a cosmology with $(h, \Omega_m, \Omega_\Lambda) = (0.7, 0.3, 0.7)$ throughout.

2. Observations and Data Reductions

The object studied in this paper was found in a parallel field observed with the ACS Wide Field Camera (WFC) during NICMOS observations of the *HST* Ultra-Deep Field (GO program 9803, PI: Thompson) in 2003 September. It was observed for 9,9,18,27 orbits in the F435W,F606W, F775W,F850LP bandpasses, respectively, hereafter referred to as B_{435}, V_{606}, i_{775}, and z_{850}. The pointing pattern was a grid of nine positions, spaced by about one NICMOS field, or $\sim 30''$. These data are public and were retrieved from the STScI archive where they received the standard CALACS on-the-fly reprocessing (OTFR) to the point of flatfielded images in units of electrons. Further processing, including cosmic ray rejection and final image combination, was performed with the "Apsis" data reduction software described in detail by Blakeslee et al. (2003a), with refinements as noted in Blakeslee et al. (2003b). Apsis now also performs automatic astrometric recalibration of the images; the resulting zero-point error is $\sim 0\farcs1$, dominated by systematic effects in the astrometric catalogues.

Two of the z_{850} exposures taken during one of the orbits were adversely affected by a bright star that landed precisely at the edge of one of the CCD chips, resulting in charge bleeding into the overscan area used in the STScI CALACS processing. This led to a large erroneous slope in the fit to the overscan, making OTFR versions of these images unusable. We chose simply to omit these two images, which reduced the final z_{850} signal-to-noise by less than 2%. The final exposure times in our summed images were then 20700 sec (B_{435}), 20679 sec (V_{606}), 41400 sec (i_{775}), and 59800 sec (z_{850}). We use photometric AB magnitude zero points in these four bands of 25.673, 26.486, 25.654, and 24.862 (Sirianni et al. 2003,

in preparation) and correct for $E(B-V) = 0.008$ mag of extinction (Schlegel et al. 1998). Finally, we obtained follow-up spectroscopy in 2003 November with the Magellan Clay 6.5-m telescope using the LDSS-2 at a dispersion of 5.3 Å pix^{-1}. The total exposure time was 7200 sec, and the data were reduced using standard techniques.

3. Analysis and Results

Figure 1 shows a composite color image constructed from a 0.′8 portion of the B_{435}, V_{606}, z_{850} images. A dramatic blue arc, subtending $\sim 120°$ is readily visible at a radius of 1.″63 perpendicular to the major axis of a red early-type galaxy. An apparent counter-arc of the same color at a radius of 0.″6 can be seen in the inset image. A number of other blue, tangentially oriented features (e.g., a faint arc to the south of the elliptical) may also be lensed. Several nearby galaxies have colors and/or photometric redshifts (see below) similar to the lensing galaxy and likely make up a group. Keeton et al. (2000) predict that 20–25% of galaxy lenses will be in groups massive enough to perturb the lensing potential. We note that this field has also been observed with Chandra (Rosati et al. 2002), and we find an upper limit to the X-ray flux of 1×10^{-15} erg cm^{-2} s^{-1} in the 0.5–2 keV band, indicating $L_X < 2 \times 10^{42}$ erg s^{-1} at the measured $z = 0.62$. The surrounding group must then be low-mass, $\lesssim 2 \times 10^{13} M_\odot$, assuming the $L_X - M$ relation from Reiprich & Böhringer (2002), although it could still have a significant effect on the lensing.

For accurate photometric and structural measurements of the arc, it is necessary to first model and subtract the light from the lensing galaxy. We used custom 2-d isophote-fitting software, masking the arcs and other nearby sources before fitting. The fitted models resulted in small residuals and indicate an effective radius $R_e \approx 1.''6$. Figure 2 illustrates the detailed knot structure that becomes apparent in the arcs following galaxy subtraction; the knot positions are given in the figure caption. A combination of the B_{435} and V_{606} images is used for this since the arcs are so blue relative to the galaxy. The main arc is brighter than the counter-arc by a factor of 7.9 ± 0.5, depending on whether or not the concentration near the south end of the main arc is counted. We tabulate our key measurements on this lensing system in Table 1. The galaxy redshift was measured from the LDSS-2 spectra using template cross-correlation, and the arc photometric redshift was estimated using "BPZ" (Benítez 2000) with revised templates from Benítez et al. (2004).

If we estimate the Einstein radius θ_E of the system to be the projected distance of the primary arc and assume a singular isothermal sphere model (e.g., Schneider, et al. 1992) with the redshifts from Table 1, then we derive a lens velocity dispersion $\sigma \approx 305$ km s^{-1}. This changes by only $\pm 3\%$ if the source redshift is varied by ∓ 0.4. Interestingly, we predict

a very similar σ from a fundamental plane (FP) analysis of the elliptical galaxy using the data in Table 1. We K-corrected our z_{850} photometry to the SDSS r band and derived a value for σ using the coefficients and methods (including luminosity evolution of $-0.85\,z$ in the K-corrected r band and conversion of the fitted R_e to an effective circular radius) from the very large field elliptical study by Bernardi et al. (2003). The result is $\sigma = 295 \pm 45$ km s^{-1}, where the error is based on the FP scatter.

We wish to investigate whether or not an elliptical galaxy of the observed luminosity can naturally produce the observed lensed features, including the counter-arc. We construct a model using a round source galaxy and the singular isothermal form of the elliptical effective lensing potential of Blandford & Kochanek (1987), parameterized by the velocity dispersion σ and an ellipticity ϵ_p. We also include an external shear component, which may arise from a host group, the bright foreground galaxies seen in Figure 1, or misalignment between the luminous galaxy and dark matter halo (Keeton et al. 1997).

Because the system is under-constrained, we fix some model parameters to reasonable values. In particular, we set $\sigma = 295$ km s^{-1} as expected from the FP and $\epsilon_p = 0.12$, or a third of the ellipticity of the light (Mellier et al. 1993). We then allow the position, orientation, and shear components to vary. We used an optimization procedure that minimizes the deviation of the delensed positions in the source plane while optimizing the gross coincidence of the model and data in the image plane. We did not include magnification weighting or detailed constraints from the internal structure of the arcs. Figure 3 shows that the model successfully reproduces the observed geometry of the bright arc and counter-arc using a single round source. The major axis of the mass ellipsoid is aligned to within 20° of the galaxy light, while the external shear axis is within 10°. We defer more detailed modeling of the lens mass distribution and internal structure of the arcs to a future work when we have better information on the source redshift and lens velocity dispersion.

4. Discussion and Summary

Early-type lensing galaxies constitute a small but unique mass-selected sample in generally low-density environments (Kochanek et al. 2000), lacking the biases inherent in luminosity selection. Kochanek et al. (2000) concluded that these galaxies have old stellar populations with formation redshifts $z_f \gtrsim 2$ and lie on the same FP as cluster ellipticals of the same redshift. However, van de Ven et al. (2003) have analyzed the FP of 26 early-type lenses and find a range in colors and ages, with formation redshifts as low as ~ 1 and slightly younger ages on average than cluster ellipticals. The new lens studied here adds to the mass-selected sample of field ellipticals, and the multi-band coverage allows for some constraint

on age. The observed ($V_{606}-i_{775}$) and ($i_{775}-z_{850}$) colors transform fairly closely to rest-frame $(U-B)_z$ and $(B-V)_z$, respectively. We find $(U-B)_z = 0.45$, $(B-V)_z = 0.85$, with $\sim \pm 0.03$ mag uncertainty in the transformations. This implies an age $\tau_L = 4.4 \pm 0.7$ Gyr from the latest solar metallicity Bruzual & Charlot (2003) models, or formation at $z_f \approx 2.0 \pm 0.5$. Thus, the population is clearly evolved, though marginally younger than derived for cluster ellipticals (e.g., van Dokkum & Franx 2001; Blakeslee et al. 2003b).

The excellent angular resolution and wide field of ACS on *HST* now makes it possible to conduct systematic optical searches for arcsecond-scale strongly lensed objects and obtain statistically meaningful results. The two Hubble Deep Fields observed with WFPC2 together produced only one probable lens candidate (Barkana et al. 1999), while the medium-deep survey (MDS) found 10 good candidates over about 130 WFPC2 fields (Ratnatunga, Griffiths & Ostrander 1999). However, the recent paper by Fassnacht et al. (2003) lists 6 probable lens candidates in ACS GOODS fields covering only about a quarter of the MDS area. The dramatic instance of lensing we report here lies in a field adjacent to the GOODS area and brings the number of likely galaxy lenses found with ACS to 7, or about 40% of the total found with *HST* in less than 15% of its lifetime. It seems likely that after a few more years, searches in ACS fields will provide the first robust optical determination of the rate of strong gravitational lensing by individual galaxies, and thus their mass function.

We have found and provided a first analysis of a clear case of strong gravitational lensing by a field, or small group, elliptical galaxy. We estimate $z \approx 2.4$ for the arc using our four-band ACS photometry and have spectroscopically measured $z = 0.62$ for the lens galaxy. Several smaller galaxies with similar colors may form a group with the lens galaxy, although the Chandra X-ray flux limit indicates this must be fairly low-mass. We have successfully modeled the arc/counter-arc system as a single round source being lensed by an isothermal ellipsoid of velocity dispersion $\sigma = 295$ km s^{-1}, the value indicated by the fundamental plane, with a modest amount of external shear that could result from neighboring or foreground galaxies. A more thorough analysis including detailed constraints on the mass distribution and source morphology would benefit from measurements of the arc redshift and lens galaxy velocity dispersion. We expect these will be forthcoming, as will discoveries and analyses of many additional lensing systems with ACS.

ACS was developed under NASA contract NAS 5-32864, and this research has been supported by NASA grant NAG5-7697. L.I., V.M., and G.H. are supported by a Chilean Conicyt Fondap grant "Center for Astrophysics." We thank our fellow ACS Team members and support staff, especially Dave Golimowski for retrieving the data and Jon McCann for writing the software used in making Figure 1.

REFERENCES

Barkana, R., Blandford, R., & Hogg, D. W. 1999, ApJ, 513, L91

Benítez, N. 2000, ApJ, 536, 571

Benítez, N. et al. 2004, ApJS, in press (astroph/0309077)

Bernardi, M. et al. 2003, AJ, 125, 1866

Blakeslee, J. P., Anderson, K. R., Meurer, G. R., Benítez, N., & Magee, D. 2003a, ASP Conf. Ser. 295, ADASS XII, ed. G. Piotto, et al. (San Francisco: ASP), 257

Blakeslee, J. P. et al. 2003b, ApJ, 596, L143

Blandford, R. D. & Kochanek, C. S. 1987, ApJ, 321, 658

Bruzual A., G. & Charlot, S. 2003, MNRAS, in press (BC03)

Chae, K.-H. et al. 2002, Physical Review Letters, 89, 151301

Fassnacht, C. D., Moustakas, L. A., Casertano, S., Ferguson, H. C., Lucas, R. A., & Park, Y. 2003, ApJ, in press

Ford, H.C., et al. 2002, Proc. SPIE, 4854, 81

Franx, M., Illingworth, G. D., Kelson, D. D., van Dokkum, P. G., & Tran, K. 1997, ApJ, 486, L75

Im, M., Griffiths, R. E., & Ratnatunga, K. U. 1997, ApJ, 475, 457

Keeton, C. R., Kochanek, C. S., & Seljak, U. 1997, ApJ, 482, 604

Keeton, C. R., Christlein, D., & Zabludoff, A. I. 2000, ApJ, 545, 129

Kochanek, C. S. et al. 2000, ApJ, 543, 131

Mellier, Y., Fort, B., & Kneib, J.-P. 1993, ApJ, 407, 33

Ratnatunga, K. U., Griffiths, R. E., & Ostrander, E. J. 1999, AJ, 117, 2010

Reiprich, T. H. & Böhringer, H. 2002, ApJ, 567, 716

Rosati, P. et al. 2002, ApJ, 566, 667

Rusin, D., Kochanek, C. S., & Keeton, C. R. 2003, ApJ, 595, 29

Schlegel, D. J., Finkbeiner, D. P., & Davis, M. 1998, ApJ, 500, 525

Schneider, P., Ehlers, J., & Falco, E. E. 1992, Gravitational Lenses (Berlin: Springer-Verlag)

van de Ven, G., van Dokkum, P. G., & Franx, M. 2003, MNRAS, 344, 924

van Dokkum, P. G. & Franx, M. 2001, ApJ, 553, 90

Table 1. Summary of Measurements

Quantity	value	±	units
	Lens Galaxy		
R.A.(J2000)	03:32:38.22	$0\farcs1$	h:m:s
Dec.(J2000)	−27:56:52.94	$0\farcs1$	°:′:″
total $z_{850,0}$	18.92	0.04	mag
$(B_{435}-V_{606})_0$	2.48	0.02	mag
$(V_{606}-i_{775})_0$	1.41	0.01	mag
$(i_{775}-z_{850})_0$	0.43	0.01	mag
R_e	$1\farcs60$	0.25	arcsec
ellipticity	0.36	0.05	...
PA	58°	4°	deg
$z_{\rm spec}$	0.6174	0.0003	$\Delta\lambda/\lambda$
	Main Arc		
total $V_{606,0}$	23.70	0.10	mag
$(B_{435}-V_{606})_0$	0.33	0.02	mag
$(V_{606}-i_{775})_0$	0.10	0.01	mag
$(i_{775}-z_{850})_0$	−0.01	0.02	mag
radius	$1\farcs63$	0.02	arcsec
length	$\gtrsim 3\farcs35$	...	arcsec
$z_{\rm phot}$	2.4	0.3	$\Delta\lambda/\lambda$

Note. — All magnitudes are AB; galaxy colors are within a $0\farcs5$ radius; PA is measured E from N. Arc "radius" refers to separation along major axis.

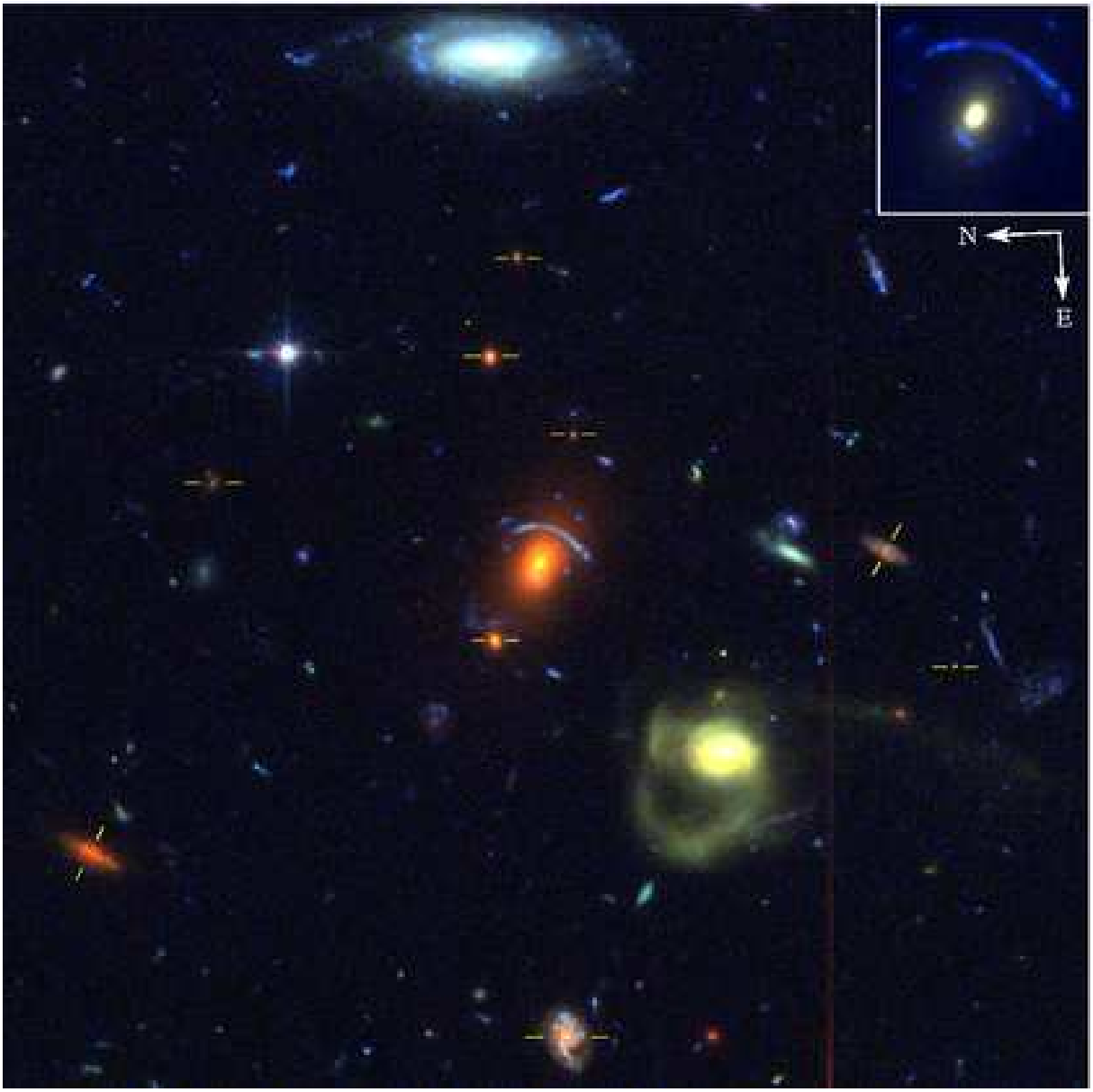

Fig. 1.— ACS/WFC $B_{435}V_{606}i_{775}$ color composite image of a 0.′8 square region centered on J033238−275653 and shown in the observed orientation. The prominent blue arc is $\sim 1.''6$ W/SW of the lens galaxy; a candidate counter-arc and additional faint arc-like features (particularly to the immediate south of the elliptical) are visible in the inset image. Galaxies having photometric redshifts with uncertainties $\lesssim 0.1$ and values within ± 0.1 of the lens galaxy are marked. The bright yellow-colored galaxy $12''$ to the SE of the lens with extended tidal arms (reaching to the edge of the figure) has a photometric redshift of 0.2.

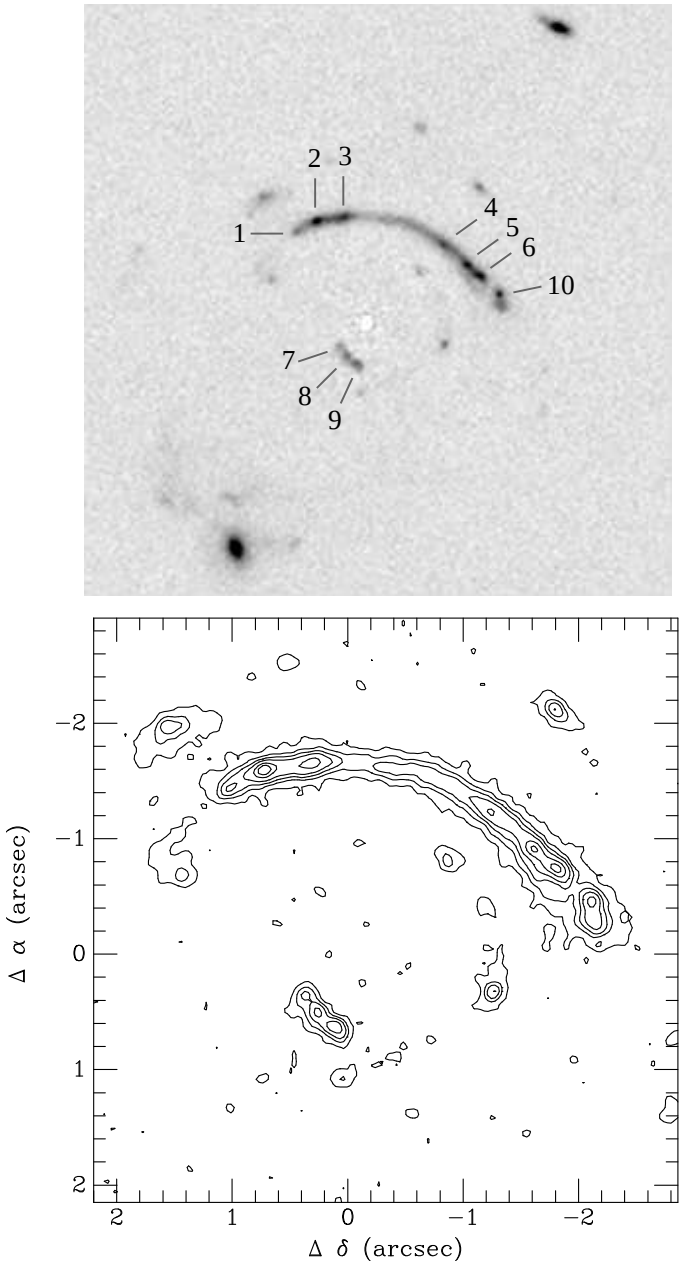

Fig. 2.— A $9'' \times 9''$ region of the B_{435}+V_{606} image ("drizzled" to $0\farcs03\,\mathrm{pix}^{-1}$ to improve the sampling) following galaxy model subtraction, with short lines labeling several bright knots in the main arc and candidate counter-arc (top). Contour plot of the central $5''$ of this region (bottom); most of the objects have elongated morphologies or tangential orientations suggestive of lensing. For reference, the precise (RA, Dec) offsets from the galaxy center for knots 1–10 are, respectively: $(-1\farcs46, 0\farcs97)$, $(-1\farcs62, 0\farcs65)$, $(-1\farcs65, 0\farcs24)$, $(-1\farcs13, -1\farcs26)$, $(-0\farcs79, -1\farcs60)$, $(-0\farcs61, -1\farcs78)$, $(0\farcs32, 0\farcs43)$, $(0\farcs48, 0\farcs33)$, $(0\farcs61, 0\farcs20)$, $(-0\farcs30, -2\farcs06)$.

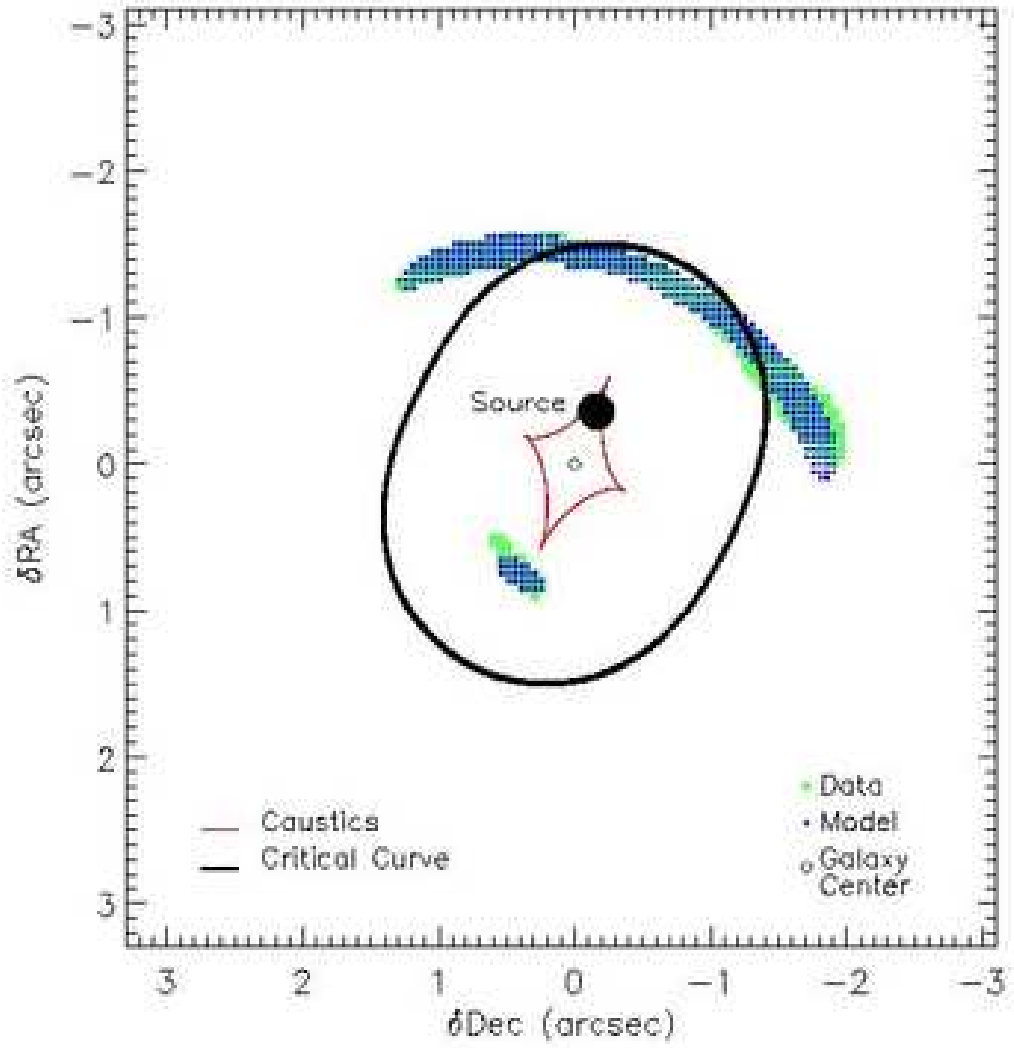

Fig. 3.— Lensing model for the J033238−275653 system. The galaxy center lies at (0,0), and the orientation is the same as in Figures 1 and 2. The caustic and critical curves are indicated in red and black, respectively. The green shading illustrates the data regions used in the modeling, while the small blue points indicate the area to which the shown source is mapped in this model.